Hydrogel-based soft pneumatic bending actuator with self-healing and proprioception capabilities

A. López-Díaz[1], A. Braic[1], F. Ramos[1], I. Payo[2], E. Vázquez[3] and A. S. Vázquez[1]*

March 10, 2022

Abstract

Proprioception is a necessary skill in robots and especially complicated in soft robots. It is commonly achieved by adding an external complement to the robotic structure that acts as a sensor. In this work, we present an approach in which the material itself (a cationic network hydrogel) serves as a structure and as a curvature sensor in a soft pneumatic bending actuator. The experiments carried out validate the use of the resistive strain capacity of our hydrogel as a proprioceptive sensor. We believe that this sensing capacity, together with the high stretchability and self-healing capability of our material makes our approach an interesting alternative for the development of soft actuators.

1 Introduction

Smart materials can be of great importance in the development of soft robotic systems. For instance, they can be used to develop soft devices with mechanical sensing capable of providing tactile and proprioceptive data. Indeed, these mechanical transducers are based on the resistive, piezoresistive, capacitive, magnetic, optical or inductive properties of the materials [1]. Usually, these sensors are integrated into the soft robot as an add-on. For example, in [2] Bilodeau et al. integrate a capacitive sensor in a bending actuator to measure its curvature. In [3], Cianchetti et al. integrate a resistive sensor on top of a soft robotic arm to obtain its shape. In [4], Chen et al. present a bending actuator that embeds an optic waveline as a curvature proprioceptive sensor. A second less common approach, which we explore in this paper, is that the same

*This work was supported by the EU 881603-Graphene Core 3 European Union (Flagship project), the Spanish Ministerio de Economía y Competitividad (project CTQ2017-88158-R), the Spanish Ministerio de Educación, Cultura y Deporte (grant FPU17/02617) and the FEDER-Junta de Comunidades de Castilla-La Mancha (project SBPL4/17/180501/000204).

†[1] Escuela Técnica Superior de Ingeniería Industrial. Universidad de Castilla-La Mancha, 13071 Ciudad Real, Spain. {antonio.ldiazcampo, francisco.ramos, andress.vazquez}@uclm.es; andrei.braic@alu.uclm.es

‡[2] Escuela de Ingeniería Industrial y Aeroespacial. Universidad de Castilla-La Mancha, 45071 Toledo, Spain. ismael.payo@uclm.es

§[3] Instituto Regional de Investigación Científica Aplicada (IRICA). Universidad de Castilla-La Mancha, 13071 Ciudad Real, Spain. ester.vazquez@uclm.es

Figure 1: Soft robotic hand with hydrogel-based pneumatic actuators.

material that forms the robotic structure serves as well as a sensor. Self-sensing ionic actuators are a good example of this approach [5]. Helps and Rossiter present in [6] another interesting approach in which a conductive liquid is used as a source of energy and a sensor for a hydraulic soft actuator.

Mechanically, materials used in soft robots must be highly stretchable. This causes serious durability problems which make self-healing polymers very appealing for its use in this field [7]. The self-healing capability is not only useful in robotic actuators to recover from damage, but also beneficial in soft sensors. Wang et al. in [8] present a relevant work on this aspect, where a highly stretchable and conductive polymer composite with self-healing capacity is used for the manufacture of strain and pressure soft sensors. Our work is aligned with this approach: we present the development of soft robotic structures (i.e. actuators) that are highly stretchable with self-healing and proprioception capabilities due to the use of our cationic network hydrogel [9].

Hydrogels have great potential in soft robotics because of their stretchability, bio-compatibility and conductivity (see [10] for a recent review). They can be used to develop actuators [11] and sensors [12]. In previous work, we have used our hydrogel to develop electric actuators [13] and self-healing actuators [14]. In this paper we present the design of a pneumatically actuated soft finger whose hydrogel structure intrinsically includes both proprioception and self-healing. The main contributions of this work are the validation of the capacity of our hydrogel as a resistive strain sensor, its use in a finger included in a soft reconfigurable robotic hand (see Fig. 1), the signal conditioning circuit, and the calibration to measure finger curvature (i.e. proprioception).

2 Hydrogel with self-healing capability and electrical properties

The hydrogel used in this work is prepared by the radical polymerization of a solution formed by [2-(acryloyloxy)ethyl]-trimethylammonium chloride (AETA) as monomer (56.05 wt%), N,N'-methylenebisacrylamide (MBA) as crosslinker (0.08 wt%), sodium 2,4,6-trimethylbenzoylphosphonate (NaTPO) as photoinitiator (0.17 wt%) and deionized water as solvent (43.70 wt%). This solution is photopolymerized under UV light (365 nm) during less than 2 minutes (the exact time depends on the amount of hydrogel and the light power).

After preparation, the hydrogel is kept under ambient conditions (25°C, 1

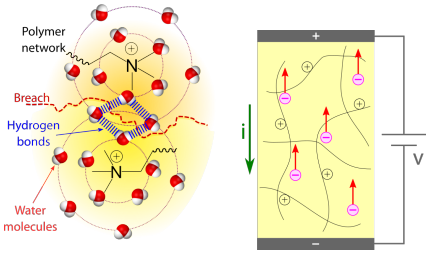

(a) Self-healing ability achieved thanks to hydrogen bonds between water molecules.

(b) Electrical conductivity due to free negative ions in the hydrogel structure.

Figure 2: Properties of our hydrogel.

atm) for at least seven days to reach the *equilibrated* state, in which the hydrogel only has a low amount of water bound to its polymeric network. Thanks to this, the hydrogel is able to self-heal in an autonomous way (without external stimulus or agents): water molecules form strong hydrogen bonds while being still bound to the polymer network, thus causing the healing (Fig. 2(a)).

Our hydrogel in equilibrated state presents a tensile Young's Modulus of 457.3 $\pm$ 32.2 kPa, an ultimate tensile strength (UTS) of 289 $\pm$ 111 kPa and a strain to failure (STF) of 9.99 $\pm$ 0.51. The healing efficiency after 24 hours is 100% in terms of Young's Modulus (complete recovery), and at least 73% in UTS and STF. More details about its mechanical properties, the self-healing mechanism and its efficiency can be found in [9, 14].

Besides this self-healing property, our hydrogel possesses electrical properties due to its cationic polymeric network. To balance positive charges bound to the network, free negative ions (chlorine, Cl^-) are released inside the structure of the hydrogel during the synthesis process (Fig. 2(b)), thus conferring electrical conductivity to the hydrogel. When an electric field is applied, these free ions move and generate a current. This property has been exploited as an actuation method in previous works [13], which benefit from the ionic mobility to drag water in a swollen hydrogel.

Since our hydrogel is a soft material and an isotropic electrical conductor, its resistance is affected by any deformation. For example, if a hydrogel sample is stretched, it will increase its length while reducing its cross section, both contributing to increase its electrical resistance. If a known current is applied to the sample, and the voltage between two points is measured, any change in the resistance will be reflected in the measurement, which can be related to the deformation. This principle is used in the curvature sensor of the actuator presented in this work. Although the expansion suffered by the hydrogel in our actuator involves changes in the geometry that complicates the theoretical analysis of the resistance, this principle can be still applied as demonstrated in the following sections.

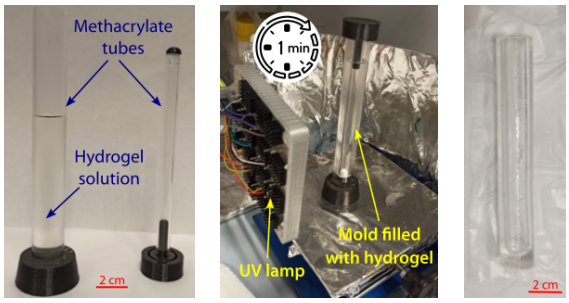

(a) Mold filling. (b) Photopolymerization. (c) Bladder.

Figure 3: Manufacturing procedure of the hydrogel bladder step by step. First, the mold is filled with hydrogel solution and the tubes are assembled (a). Second, the photopolymerization process takes approximately 1 min (b). After that, the bladder is extracted from the mold (c).

3 Hydrogel-based pneumatic actuator

The actuator presented in this work consists of a cylinder shaped bladder with a shell reinforcement to achieve a bending actuation. This geometry is similar to the soft pneumatic actuator presented in [15].

Fabrication is divided in two steps. First, our hydrogel is polymerized to create a bladder that can be actuated pneumatically. Its manufacturing process, illustrated in Fig. 3, uses a mold, consisting of two concentric methacrylate tubes, which is filled with the hydrogel solution and then photopolymerized for 1 min, as explained in the previous section. The equilibrated bladder is a cylinder of 18 mm outer diameter with a concentric cavity of 10 mm diameter.

Second, this bladder is rolled in a 3D-printed reinforcement of a flexible material (Recreus FilaFlex™) that prevents excessive radial expansion of the hydrogel bladder, and guides the bending movement of the actuator. Different parameters of the reinforcement's geometry were studied, and the best overall results were obtained with a design of 20 stripes of 3.5 mm width, separated by 1 mm, and 0.8 mm thickness (Fig. 4(a)). With this design, an actuator curvature of $\sim$270° was obtained at $\sim$0.42 bar (Fig. 4(b)).

The reinforcement also contains the electrodes of the sensing system, which measures the actual curvature in different points of the actuator. Six electrodes are installed: four of them, equispaced, measure curvature in three regions of the actuator, while the terminal ones inject the current into the hydrogel. These electrodes are manufactured with layers of copper tape placed along certain stripes of the reinforcement as shown in Fig. 4(c). Finally, a JST-XH plug is used to connect the sensors to the signal conditioner. Fig. 4(d) shows the final appearance of the actuator. The details on the sensor and the required instrumentation are presented in the following section.

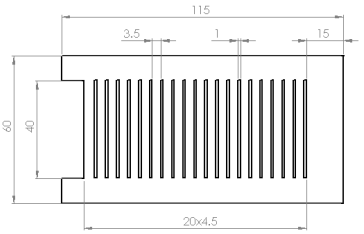

(a) Design of the 3D-printed reinforcement.

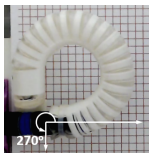

(b) Reinforcement design working at 0.42 bar.

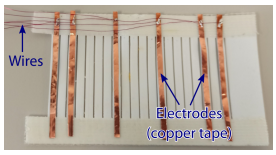

(c) Electrodes installation on the transversal strips of the 3D-printed reinforcement.

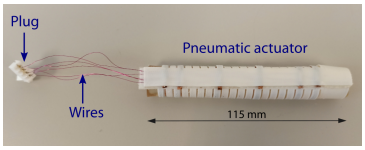

(d) Soft bending actuator with proprioceptive sensor.

Figure 4: Reinforcement design, installation, and resulting actuator.

4 Curvature sensor and instrumentation

Since the curvature of the actuator previously shown is achieved through a deformation in the hydrogel inner bladder, it is reasonable to take advantage of its ionic conductivity in order to measure the curvature. The working principle is the same previously explained in section 2: the higher the expansion of the bladder, the higher the electrical resistance of the hydrogel (more length, lower section) and the higher the actuator curvature.

A proper conditioning circuit needs to be designed to fulfill this purpose. The circuit presented here is based on the work of I. Payo et al. [16], in which a signal conditioning circuit for strain sensors using acrylamide hydrogels and organogels with DMSO solvent is developed. Instead of these gels, we have used our hydrogel to build our actuator because of its self-healing ability. Therefore, in this work we have adapted and verified a conditioning circuit (shown in Fig. 5) for our cationic network hydrogel. The full-wave rectifier in [16] has been substituted by a precision half-wave rectifier to prevent the voltage drops caused by the diodes. As long as the signal frequency is large enough, the output voltage of the rectifier will be properly stable in the hold capacitor (C_{conv}).

The first stage of the circuit injects an alternating current (i) of frequency f ($\omega = 2\pi f$) along the hydrogel between the two outer electrodes (e_1 and e_2):

$$i = \frac{v_{in}}{R} = \frac{V_{in} \cdot sin(\omega t)}{R} \tag{1}$$

The use of alternating current (AC) is important, because with direct current (DC) we would obtain an actuation behavior similar to the one in [13]: the free ions drag water with them, originating a gradient in the swelling distribution inside the network that causes a dishomogeneity in the material. Besides, the large displacements of the ions introduces non-linearities in the electrical

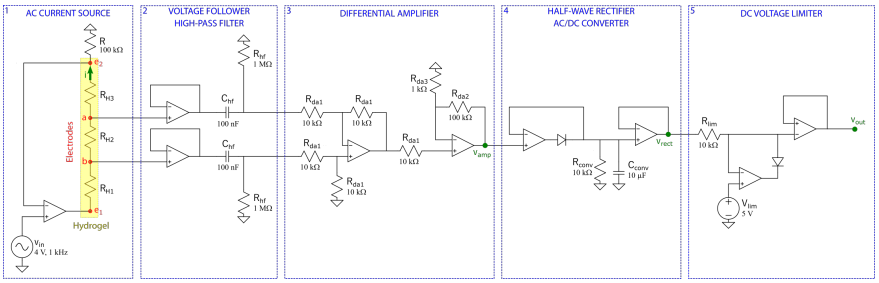

Figure 5: Schematic of the signal conditioning circuit with all the stages. Only a pair of inner measuring electrodes is depicted, so stages 2-5 need to be implemented for every measurement pair, while stage 1 is common for all of them.

behavior. These undesirable effects are overcome by using alternating current.

Since the current flows between the outer electrodes, a voltage measurement can be taken in a pair of inner electrodes, denoted as a and b in Fig. 5. This technique, known as four probe method, provides better outcomes than the two probe method (only one pair of electrodes for both injecting and measuring), which introduces errors in the case that the electrodes-sample interface impedance cannot be neglected [16].

As mentioned in the previous section, we include four inner equispaced electrodes (Fig. 4(c)) to measure the curvature in three zones of the actuator. Although the theoretical curvature of our actuator is constant, we consider that having different measurements along the actuator can add valuable information in some cases; for example, if there is a contact in the middle of the actuator that alters the curvature shape.

Only one current source is needed (stage 1), but the stages 2-5 of the circuit (Fig. 5) need to be repeated for each pair of inner electrodes to condition the voltage measurement v_{ba}:

$$v_{ba} = v_b - v_a = i \cdot R_{H2} \tag{2}$$

The aim of stage 2 is to isolate electrically the hydrogel from the rest of the circuit. This is achieved with operational amplifiers (op-amps) in voltage follower configuration. Furthermore, a high-pass filter is included in this stage to cancel unwanted offset in the output of the op-amps.

Stage 3 is a differential amplifier whose objective is to amplify the voltage measured between the electrodes:

$$v_{amp} = v_{ba}\frac{R_{da2}}{R_{da3}} = \frac{V_{in} \cdot sin(\omega t) \cdot R_{H2}}{R}\frac{R_{da2}}{R_{da3}} \tag{3}$$

The amplified signal is rectified by using an op-amp and a diode, and converted from AC to DC in stage 4:

$$v_{rect} = V_{in}\frac{R_{H2}}{R}\frac{R_{da2}}{R_{da3}} \tag{4}$$

The final stage of the circuit is a voltage limiter whose goal is to protect the data acquisition system used to record the output of the circuit (v_{out}):

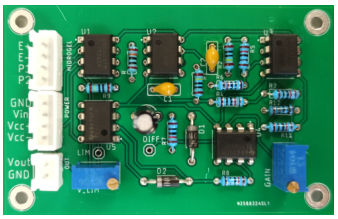

Figure 6: Signal conditioning circuit manufactured in a PCB.

$$v_{out} = \begin{cases} v_{rect} = V_{in} \frac{R_{H2}}{R} \frac{R_{da2}}{R_{da3}} & \text{if } v_{rect} < V_{lim} \\ V_{lim} & \text{if } v_{rect} \geq V_{lim} \end{cases} \tag{5}$$

In our case, the input is set to 4 V and 1 kHz, while the voltage limitation is set at 5 V (we use Arduino to read v_{out}). The values of the resistors and capacitors, shown in the schematic of Fig. 5, were adapted to the material and the geometry of the actuator in order to obtain a proper performance in the actuator working region.

Substituting the appropriate values in (5) and considering that v_{rect} is lower than 5 V, the output of the circuit is:

$$v_{out} = V_{in} \frac{R_{H2}}{R} \frac{R_{da2}}{R_{da3}} = 4R_{H2} \tag{6}$$

where the units of v_{out} and R_{H2} are in volts and kilohoms, respectively. As can be seen, the relation between the output and the measured resistance is linear. This signal conditioning circuit was manufactured in a PCB, as shown in Fig. 6.

5 Experimental validation

The verification of the proprioceptive capacity of the actuator to measure its curvature (i.e. inverse of radius of curvature), the calibration of the sensor, its stability over time and the effect of breaks and healing have been carried out through the experimentation described in this section. For this purpose, an experimental platform has been designed capable of applying a precise pressure to the actuator and calculating its curvature by means of computer vision (Fig. 7). This curvature is assumed to be homogeneous along the actuator in all tests.

5.1 Proprioception and calibration

As explained in the previous section, the actuator contains four electrodes that make it possible to measure the deformation in three different sections of the actuator. To check if there is a deterministic relationship between the voltage measured by the sensors and the curvature of the actuator, a series of repeated experimental tests has been carried out. These tests consist of compression-decompression cycles between [0, 0.45] bar with steps of 0.05 bar. The curvature in each step was calculated through image processing and related to the sensor measurement.

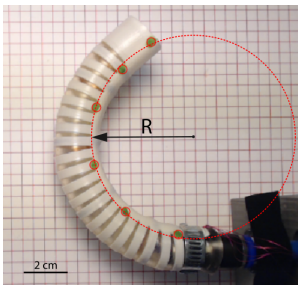

Figure 7: Automatic detection of markers and adjustment of the circumference through image processing.

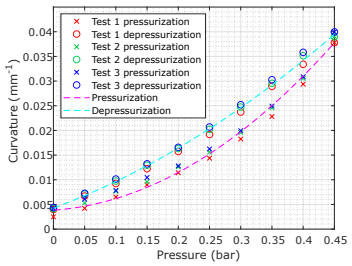

(a) Actuator response. Curvature/pressure experimental data.

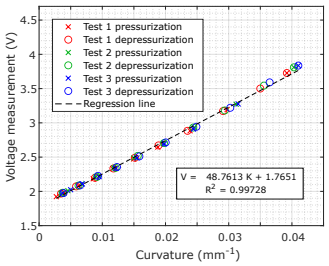

(b) Sensor response. Output voltage/curvature experimental data and regression line.

Figure 8: Experimental tests for three compression-decompression cycles. All the data correspond to the same actuator and the same pair of electrodes. As can be seen in (b), the voltage/curvature points fit almost perfectly to the regression line.

The mechanical response of the actuator (i.e. curvature vs. input pressure) is plotted in Fig. 8(a), showing the typical hysteresis of this kind of actuators between pressurization and depressurization cycles. Fig. 8(b) shows the sensor output for a specific pair of electrodes. As can be seen, there is a repeatability between the voltage measurements and the actual curvature of the actuator, without observing hysteresis in the curvature-voltage correlation, despite the mechanical hysteresis caused by the hydrogel and seen in Fig. 8(a).

Fig. 9 shows a comparison of the measurements obtained for the three sections in the same set of experiments. As can be seen, the curvature-voltage slopes vary slightly between sections. This may be due to small manufacturing differences (i.e. distance between electrodes) or a non-constant curvature along the actuator.

However, the linearity and repeatability of the results allows the regression line for each pair of electrodes to serve as a calibration for the sensor while verifying the viability of the material as a proprioceptive sensor.

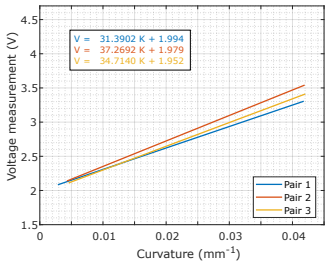

Figure 9: Voltage/curvature characteristic for the three sections of the same actuator. Each line is obtained by a linear correlation ($R^2 > 0.99$) over the data of three compression-decompression cycles (like in Fig. 8(b)).

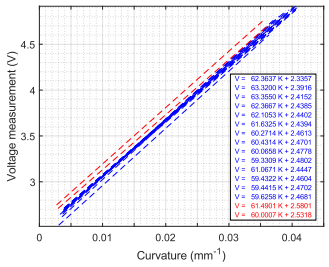

Figure 10: Voltage/curvature characteristic for the same pair of electrodes at different times. The order of the tests follows the legend. Blue tests are carried out every 15 minutes. Red tests are carried out every 4 hours after the blue ones. Each line is obtained by a linear correlation ($R^2 > 0.98$) over the data of three compression-decompression cycles.

5.2 Stability

Although the material is in equilibrium, the change in atmospheric conditions over time can slightly influence its swelling degree and therefore its performance (i.e. curvature acquired at a given pressure) which can also affect sensor measurements. In Fig. 10 a total of 14 trials over the same pair of electrodes can be seen in blue with a difference of 15 min between each one. The tests in red were performed after the last 15 min test within intervals of 4 hours. This makes an experiment of about 12 hours in which the actuator was affected by ambient conditions.

The test results show that indeed the sensor measurements vary slightly over time, without noticing a significant trend in the evolution of the lines. However, the linearity in each of them is maintained ($R^2 > 0.98$), which makes the recalibration process extremely simple, since the regression line can be easily obtained by knowing the points of maximum and minimum curvature of the actuator. These points can be mechanically established, eliminating the need for an image processing system for the recalibration process.

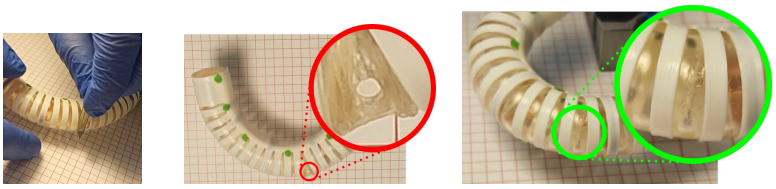

(a) Cut performed over the hydrogel bladder.

(b) Damaged actuator after being cut.

(c) After 24 h, the hydrogel inner bladder is self-healed.

Figure 11: Damage and self-healing processes.

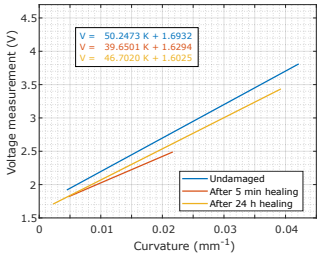

Figure 12: Voltage/curvature characteristic for an undamaged, damaged and healed actuator. All the lines correspond to the same pair of electrodes. Each line is obtained by a linear correlation ($R^2 > 0.94$) over the data of three compression-decompression cycles.

5.3 Influence of breakage and healing

The influence of breaks and subsequent self-healing on the sensor curvature measurements were analyzed with several tests in which the actuator was cut with a scalpel (see Fig. 11). To quantify this influence, every compression test was performed twice: allowing 5 min of healing and allowing 24 hours of healing. Fig. 12 shows a representative result of the experiments performed. As can be seen, the sensor works the same for virgin or healed actuators, being able to detect that the healed actuator breaks in the test performed at 5 min, while after 24 hours of healing detects a point of maximum curvature without breaking. While it is possible that the difference in starting curvatures and slopes between blue and yellow measurements is due to environmental changes over time, it cannot be ruled out that it is also due to the effect of cutting. This point must be verified in future works.

6 Discussion and conclusions

In this work we present a soft pneumatic bending actuator with proprioceptive and self-healing capacities. This actuator can be used as a finger on a robotic hand, as shown in Fig. 1. The design of the actuator is not really new, since it corresponds to a widely used configuration of reinforced pneumatic actuators. The real contribution of this work is the validation of our hydrogel as a material

that allows proprioception and the design of the conditioning circuit that makes it possible. We believe that this proprioception, together with the mechanical and self-curing capabilities of our hydrogel, make this material an interesting alternative to soft systems in which sensorization is included as an *add-on* to the robotic structure. In our approach, the hydrogel itself forms the soft structure while allowing actuation (thanks to its high stretchability) and sensorization (thanks to its electrical conductivity), thus enabling a more compact design.

Although the tests carried out demonstrate the validity of our approach, a more detailed study is still needed, especially on how environmental conditions (i.e. change in the hydrogel swelling) affect the behavior of the whole actuator-sensor system. Besides, further studies should be done to analyze the sensor response to desired contacts in the structure (i.e. grasped object) or external perturbations (forces) that can cause unwanted deformations and motions of the actuator.

References

[1] H. Wang, M. Totaro, and L. Beccai, "Toward perceptive soft robots: Progress and challenges," vol. 5, no. 9, p. 1800541, jul 2018.

[2] R. A. Bilodeau, M. C. Yuen, J. C. Case, T. L. Buckner, and R. Kramer-Bottiglio, "Design for control of a soft bidirectional bending actuator," in *2018 IEEE/RSJ International Conference on Intelligent Robots and Systems (IROS)*. IEEE, 2018, pp. 1–8.

[3] M. Cianchetti, F. Renda, A. Licofonte, and C. Laschi, "Sensorization of continuum soft robots for reconstructing their spatial configuration," in *2012 4th IEEE RAS & EMBS International Conference on Biomedical Robotics and Biomechatronics (BioRob)*. IEEE, 2012, pp. 634–639.

[4] W. Chen, C. Xiong, C. Liu, P. Li, and Y. Chen, "Fabrication and dynamic modeling of bidirectional bending soft actuator integrated with optical waveguide curvature sensor," *Soft robotics*, vol. 6, no. 4, pp. 495–506, 2019.

[5] K. Kruusamäe, A. Punning, A. Aabloo, and K. Asaka, "Self-sensing ionic polymer actuators: a review," in *Actuators*, vol. 4, no. 1. Multidisciplinary Digital Publishing Institute, 2015, pp. 17–38.

[6] T. Helps and J. Rossiter, "Proprioceptive flexible fluidic actuators using conductive working fluids," *Soft robotics*, vol. 5, no. 2, pp. 175–189, 2018.

[7] S. Terryn, J. Langenbach, E. Roels, J. Brancart, C. Bakkali-Hassani, Q.-A. Poutrel, A. Georgopoulou, T. G. Thuruthel, A. Safaei, P. Ferrentino, T. Sebastian, S. Norvez, F. Iida, A. W. Bosman, F. Tournilhac, F. Clemens, G. V. Assche, and B. Vanderborght, "A review on self-healing polymers for soft robotics," vol. 47, pp. 187–205, jul 2021.

[8] T. Wang, Y. Zhang, Q. Liu, W. Cheng, X. Wang, L. Pan, B. Xu, and H. Xu, "A self-healable, highly stretchable, and solution processable conductive polymer composite for ultrasensitive strain and pressure sensing," *Advanced Functional Materials*, vol. 28, no. 7, p. 1705551, 2018.

[9] A. Naranjo, C. Martín, A. López-Díaz, A. Martín-Pacheco, A. M. Rodríguez, F. J. Patiño, M. A. Herrero, A. S. Vázquez, and E. Vázquez, "Autonomous self-healing hydrogel with anti-drying properties and applications in soft robotics," *Applied Materials Today*, vol. 21, p. 100806, dec 2020.

[10] Y. Lee, W. Song, and J.-Y. Sun, "Hydrogel soft robotics," *Materials Today Physics*, vol. 15, p. 100258, 2020.

[11] L. Ionov, "Hydrogel-based actuators: possibilities and limitations," *Materials Today*, vol. 17, no. 10, pp. 494–503, 2014.

[12] X. Sun, S. Agate, K. S. Salem, L. Lucia, and L. Pal, "Hydrogel-based sensor networks: Compositions, properties, and applications—a review," *ACS Applied Bio Materials*, vol. 4, no. 1, pp. 140–162, 2020.

[13] A. López-Díaz, A. Martín-Pacheco, A. M. Rodríguez, M. A. Herrero, A. S. Vázquez, and E. Vázquez, "Concentration gradient-based soft robotics: Hydrogels out of water," *Advanced Functional Materials*, vol. 30, no. 46, p. 2004417, sep 2020.

[14] A. Lopez-Diaz, A. Martin-Pacheco, A. Naranjo, C. Martin, M. A. Herrero, E. Vazquez, and A. S. Vazquez, "Autonomous self-healing pneumatic

McKibben muscle based on a new hydrogel material," in *2020 3rd IEEE International Conference on Soft Robotics (RoboSoft)*. IEEE, may 2020.

[15] G. Agarwal, N. Besuchet, B. Audergon, and J. Paik, "Stretchable materials for robust soft actuators towards assistive wearable devices," *Scientific Reports*, vol. 6, p. 34224, sep 2016.

[16] I. Payo, J. L. Polo, B. López, D. Serrano, A. M. Rodríguez, M. A. Herrero, A. Martín-Pacheco, I. Sánchez, and E. Vázquez, "Signal conditioning circuit for gel strain sensors," *Smart Materials and Structures*, 2021, to be published.